BRAIN CONNECTIVITY
Volume 4, Number 6, 2014

DOI: 10.1089/brain.2013.0195

Time of Acquisition and Network Stability in Pediatric Resting-State Functional Magnetic Resonance Imaging

Tonya White,[1,2] Ryan Muetzel,[1,3] Marcus Schmidt,[1] Sandra J.E. Langeslag,[1] Vincent Jaddoe,[3,4] Albert Hofman,[3,4] Vince D. Calhoun,[5,6] Frank C. Verhulst,[1,3] and Henning Tiemeier[1,3,4]

Abstract

Resting-state functional magnetic resonance imaging (rs-fMRI) has been shown to elucidate reliable patterns of brain networks in both children and adults. Studies in adults have shown that rs-fMRI acquisition times of ~5 to 6 min provide adequate sampling to produce stable spatial maps of a number of different brain networks. However, it is unclear whether the acquisition time directly translates to studies of children. While there are many similarities between the brains of children and adults, many differences are also evident. Children have increased metabolism, differences in brain morphology and connectivity strengths, greater brain plasticity, and increased brain noise. Furthermore, there are differences in physiologic parameters, such as heart and respiratory rates, and compliance of the blood vessels. These developmental differences could translate into different acquisition times for rs-fMRI studies in pediatric populations. Longer scan times, however, increase the subject burden and the risk for greater movement, especially in children. Thus, the goal of this study was to assess the optimum acquisition time of rs-fMRI to extract stable brain networks in school-age children. We utilized fuzzy set theory in 84 six-to-eight year-old children and found that eight networks, including the default mode, salience, frontal, left frontoparietal, right frontoparietal, sensorimotor, auditory, and visual networks, all stabilized after ~5½ min. The sensorimotor network showed the least stability, whereas the salience and auditory networks showed the greatest stability. A secondary analysis using dual regression confirmed these results. In conclusion, in young children with little head motion, rs-fMRI acquisition times of ~5½ min can extract the full complement of brain networks.

Key words: acquisition time; children; independent component analyses; network stability; resting-state fMRI

Introduction

THE LAST SEVERAL YEARS HAVE witnessed a growing interest in studying developmental differences in the brain's functional network architecture (Fair et al., 2008; Supekar et al., 2010; Uddin, 2011; Vogel et al., 2010; Wu et al., 2013; Zhong et al., 2013). Functional connectivity is defined as the temporal dependency of neuronal activation patterns of anatomically separated brain regions and can be studied using resting-state functional magnetic resonance imaging (rs-fMRI) (Biswal et al., 1995). rs-fMRI is highly suitable for studying neurodevelopment of functional connectivity, since resting-state data acquisition requires minimal task demands and can yield an array of reproducible brain networks (Beckmann et al., 2005; Smith et al., 2009; van den Heuvel and Hulshoff Pol, 2010; Vogel et al., 2010). In adults, analysis of incremental durations of data acquisition times ranging from 2 to 12 min show that functional connectivity estimates stabilize after ~5 to 6 min of data collection (Franco et al., 2013; Liao et al., 2013; Van Dijk et al., 2010; Whitlow et al., 2011). To our knowledge, there have been no studies examining the minimum number of volumes or acquisition time to obtain stable functional resting-state connectivity patterns in children.

There are a number of reasons why studies of the optimal acquisition time/volumes in adults may not directly translate to studies in children. Studies have shown age-related differences between short- and long-range connections, with

Departments of [1]Child and Adolescent Psychiatry, [2]Radiology, and [4]Epidemiology, Erasmus University Medical Centre—Sophia Children's Hospital, Rotterdam, The Netherlands.
[3]The Generation R Study Group, Erasmus University Medical Centre—Sophia Children's Hospital, Rotterdam, The Netherlands.
[5]Department of Electrical and Computer Engineering, University of New Mexico, Albuquerque, New Mexico.
[6]Mind Research Network, University of New Mexico, Albuquerque, New Mexico.

long-range connections showing greater strength in adults (Fair et al., 2008). Furthermore, networks related to higher order executive functions have been shown to be less mature in children (de Bie et al., 2012). Greater immaturity could reflect less network stability. In addition, there are developmental differences in noise patterns found within the brain (McIntosh et al., 2010). Increased noise in children may be associated with the shifting of cognitive states, which may in turn result in age-related differences in the measurement of brain network stability. Finally, the studies of brain network stability with respect to volumes or time of acquisition have primarily focused on the default mode (Franco et al., 2013; Van Dijk et al., 2010) and attention networks (Van Dijk et al., 2010), and thus the stability of other brain networks is less clear.

Currently, there is considerable variation in the acquisition time used in rs-fMRI studies in children. Studies of resting-state networks in children using similar repetition times (TR) have acquisition times ranging from less than 5 min to nearly 9½ min (de Bie et al., 2012; Fair et al., 2009; Gordon et al., 2011; Jolles et al., 2011; Langeslag et al., 2013; Stevens et al., 2009; Supekar et al., 2010; Thomason et al., 2011). It has been shown in adult studies that $\sim$5 to 6 min of data yield a sufficient signal-to-noise ratio to model brain networks, whereas this has not been explored in children. Longer scan times can place an increased burden on the participants and also increase the risk for greater motion artifacts, especially in children.

Thus, our primary research question was to determine the optimal acquisition time of rs-fMRI data needed to obtain stable resting-state brain networks in school-age children. Our goal was to assess not only the stability of multiple brain networks with respect to time, but also to explore the stability of common noise components. There have been no studies to date that have evaluated the relationship between acquisition time and network stability evaluating a comprehensive group of brain and noise networks. Shorter acquisition times are important to decrease the participant burden and to reduce the chance for movement artifacts (Van Dijk et al., 2012), which are especially relevant when imaging young children (Power et al., 2012). However, there is a cost/benefit ratio in that sequences that are too short and will result in a failure to adequately model the time series associated with different networks. Thus, we sought to determine the optimal scan acquisition time to determine stable brain networks in school-age children.

Materials and Methods

Participants

The study sample included the first 188 children between the ages of six to eight who were recruited from the Generation R Study and who received an 8 min 20 sec rs-fMRI scan. The Generation R Study is a large population-based study from fetal life until young adulthood in Rotterdam, the Netherlands (Jaddoe et al., 2006; Tiemeier et al., 2012). Children were excluded if they had a contraindication in obtaining a magnetic resonance imaging (MRI) scan, suffered a major head injury, or had a neurological disorder (i.e., seizure disorder, tuberous sclerosis, history of brain tumors, etc.), or had a history of claustrophobia. Subjects included 13 children whose mothers smoked cigarettes during pregnancy, 5 children whose mothers smoked cannabis during pregnancy, 21 children whose mothers reported depressive symptoms during pregnancy, and 5 children whose mothers took selective serotonin reuptake inhibitors during pregnancy. IQ was estimated using the Mosaics and Categories subtest of the Snijders-Oomen Non Verbal Intelligence Test–Revised (Tellegen et al., 2005). The study was approved by the Medical Ethical Committee of the Erasmus Medical Center, Rotterdam.

Imaging protocol

The study design of the imaging component within the Generation R Study has been described in detail elsewhere (White et al., 2013). In brief, the children were first familiarized with the MRI scanning environment during a mock scanning session. The mock scanning session allowed the children to experience the physical environment of the scanner, including listening to recorded sounds of the actual scanner. Following the mock scanning session, MRI scans were obtained using a GE Discovery 3 Tesla scanner (General Electric, Milwaukee, WI) and an 8-channel head coil. For anatomical reference, a high-resolution T_1 inversion recovery fast spoiled gradient recalled (IR-FSPGR) sequence was obtained with the following scan parameters: TR = 10.3 msec, TE = 4.2 msec, flip angle = 16°, and 186 slices with a slice thickness of 0.9 mm and an in plane resolution of 0.9×0.9 mm. The children were able to watch a film of their choice during the high-resolution structural scan. During the rs-fMRI, the movie was turned off and the children were instructed to lie completely still with their eyes closed and to think about nothing in particular. Heart rate and respiratory rate were not collected during the scan. The rs-fMRI was obtained using an echo-planar imaging sequence sensitive to blood oxygen level-dependent contrast. The scan parameters were as follows: TR = 2000 msec, TE = 30 msec, flip angle = 85°, number of slices = 37, slice thickness = 4 mm, in-plane resolution = 3.6×3.6 mm, and number of volumes = 250.

Preprocessing

The functional images were preprocessed using a combination of analysis of functional neuroimages (AFNI, http://afni.nimh.nih.gov/) (Cox, 2012) and FSL's FMRIB's Software Library (FSL, FMRIB Software Library; FMRIB, Functional Magnetic Resonance Imaging of the Brain; www.fmrib.ox.ac.uk/fsl) (Jenkinson et al., 2012). Slice timing correction and motion correction were performed using AFNI. The functional data were spatially smoothed using AFNI with an 8-mm full width at half-maximum Gaussian kernel (White et al., 2001). Functional images were co-registered to the structural image and both the functional and structural images were normalized using the Montreal Neurological Institute T1 template (MNI152, voxel size = $2 \times 2 \times 2$ mm) using FSL's FLIRT (Jenkinson and Smith, 2001; Jenkinson et al., 2002). Two subjects lacked full brain coverage and were removed from the analyses.

Independent component analyses

The first four volumes of the resting-state functional MRI scan of each subject were discarded to allow for equilibration effects. The group independent component analysis of fMRI toolbox (GIFT) version 1.3h (http://mialab.mrn.org/

software/gift) was used to perform independent component analysis (ICA) (Calhoun and Adali, 2012; Calhoun et al., 2001) on the remaining volumes (corresponding to a data acquisition duration of 8 min 12 sec). The dimensionality was set at 16 components based on our prior work (Langeslag et al., 2013) and also supported by studies that show that the use of a higher dimensionality in children results in the splitting of the frontal component of the default mode network (DMN) (de Bie et al., 2012). The 16 components from the ICA analysis were individually assessed to determine whether they constituted a well-defined brain network or noise. Well-defined networks constitute those networks that have been consistently reported in the literature (Allen et al., 2011; Beckmann et al., 2005; Damoiseaux et al., 2006; de Bie et al., 2012; Jolles et al., 2011; Smith et al., 2009; Thomason et al., 2011; van den Heuvel and Hulshoff Pol, 2010) and include the DMN, the salience network, the frontal network, the left frontoparietal network, the right frontoparietal network, the sensorimotor network, the auditory network, and the visual network.

To assess the temporal stability of these brain networks, the dimensionality of 16 was fixed and group ICA were run on subjects after iteratively clipping off 5 TRs (10 sec) from the end of each rs-fMRI run. This was performed from 246 TRs down to 26 TRs, with the latter corresponding to a total duration of 52 sec. For the reference resting-state run (246 TRs) and for each 10-sec (5 TR) decrement, brain-wide z-maps were computed independently for each of the 16 components. The z-score reflects the degree to which the time series of each voxel within the brain map is associated with the mean time series of that specific component.

Time-based stability of the rs-fMRI components

Fuzzy set theory was used for the automated matching of components and to assess the stability of the selected rs-fMRI components over time. A fuzzy classifier (Zadeh, 1965) using a lower threshold of $z = 1.96$ and an upper threshold of $z = 2.3$ was applied to each of the component maps to yield a spatial mask for each brain component. Voxels greater than 2.3 were assigned the value 1, whereas values between 1.96 and 2.3 received a linear weighting between 0 and 1. The elements of set A_j are defined within the reference rs-fMRI as those voxels in 3D space that exceeds the threshold of 1.96, these are weighted between zero and one. The subscript refers to the number of volumes used in the comparison. In the case of the reference set, j is fixed at 246 volumes. The elements of set A_k have the same $z = 1.96$ to $z = 2.3$ fuzzy threshold as the baseline condition, except in this case A_k relates to the iterative decrements in the number of TRs ($k = 246, 241, 236, \ldots, 26$). The spatial overlap ($\varphi$) between A_j and A_k for each component was defined by Equation 1 (Kung et al., 2007):

$$\varphi = \frac{A_j \cap A_k}{A_j \cup A_k} \quad (1)$$

Dual regression analyses

In addition to analyzing the group ICA components, we also performed iterative dual regression analyses described by Beckmann et al. (2009) and performed using MATLAB (Mathworks, Natick, MA). We first regressed the set of sixteen spatial component maps individually into each subject's 4D space/time dataset. This results in a set of subject-specific time series, one per group-level spatial map. Next, the individual time series were used as temporal regressors back into the same individual's 4D space/time dataset. This was performed iteratively while chopping off 5 TR's (10 sec) and comparing the spatial maps individually from the shortened time series with the full length time series using the fuzzy approach defined in Equation 1.

Statistical analyses

The comparison between individuals who were included in the analyses and those who were dropped due subject motion or other artifacts were performed using either χ^2, *t*-tests, and a repeated-measures analysis of variance (ANOVA). A repeated-measures ANOVA was performed to assess differences between the network and noise components as the between-group factors and the overlap over time as repeated-measures within group factors.

Results

Subject motion

Our first step was to assess whether the motion artifacts remained relatively constant across the entire rs-fMRI run. This was performed in the group of 188 subjects with good registration and who had an 8 min 20 sec rs-fMRI. While motion will induce noise in the connectivity analyses (Power et al., 2012; Satterthwaite et al., 2012; Van Dijk et al., 2012), we wanted to exclude subjects who had differences in motion over time. To assess this, first the TR-to-TR translational motion for each subject was calculated using the AFNI motion correction output parameter file. The TR-to-TR translational movement parameters (x, y, and z combined using the Pythagorean theorem) for each individual were fit to a line using a MATLAB first-order polynomial function (polyfit). The slope of this line for each subject was extracted and a one-sided *t*-test was performed to assess whether the mean slope for the group differed from zero. The whole group of 188 subjects showed a significant positive slope (Mean 0.002, SD 0.004, $t = 4.7$, df 185, $p < 0.0001$) indicating that children had greater movement over time. This was also confirmed using a repeated-measures ANOVA ($F_{(9,1665)} = 7.0$, $p < 0.0001$). Then, beginning with only children who had less than 1-mm total head movement, and incrementing by 1-mm total head movement (i.e., only children who had less than 2-mm total head movement, then only children who had less than 3-mm head movement), *t*-tests were performed to assess the maximum level of movement that showed no significant positive slope. While movement less than 3 mm did not show a significant difference in slope, a maximum movement threshold of less than 4 mm did show a significant difference in slope (Mean 0.0001, SD 0.00004, $t = 2.4$, df 97, $p < 0.02$). This quantitatively derived threshold for movement less than 3 mm is very similar to that used in the literature (Gordon et al., 2011) and in our prior studies (Langeslag et al., 2013; van den Bosch et al., 2014; White et al., 2011, 2012). These findings were repeated using a repeated-measures ANOVA, which found no significant difference over time with less than 3 mm

Table 1. Demographic Characteristics for the Children and Their Parents

	Less than 3-mm head motion (n = *84*)	*Greater than 3-mm head motion or poor registration* (n = *104*)	p-*Value*
Age at MRI (years)	7.1 ± 0.58	7.0 ± 0.53	n.s.
Gender (males/females)	43/42	52/52	n.s.
Handedness (right/left/mixed)	79/5/0	95/8/1	n.s.
Nonverbal IQ	102 ± 14	101 ± 13	n.s.
Ethnicity			
Dutch or Western	57	56	n.s.
Non-Dutch/Non-Western	28	47	
Family income			
< 1,200 euro/month	12	22	n.s.
1,200 to 2,400 euro/month	21	28	
> 2,400 euro/month	52	53	
Maternal educational level (%)			
Primary	14	20	n.s.
Secondary	53	65	
Higher	18	18	
Maternal age at intake	30.5 ± 5.0	29.3 ± 5.3	n.s.
Maximum head displacement (mm)	1.5 ± 0.70	14.7 ± 15.9	n.a.

p-Values were obtained using two sample *t*-tests for continuous variables and chi-square for categorical variables.
MRI, magnetic resonance imaging; n.s., not significantly different; n.a., not applicable as this variable was used to separate the groups.

maximum movement ($F_{(9,747)} = 1.6$, $p = 0.12$), whereas it was at $F_{(9,873)} = 7.0$, $p = 0.055$ for maximum movement less than 4 mm. Further analyses were run with a total of 84 subjects who had less than 3 mm of motion. Table 1 displays the demographic characteristics for these 84 subjects and the comparison with the whole group of 188. Figure 1 shows the mean movement over time for different levels of maximum translational displacement.

Participant characteristics

The characteristics of the children who were included compared to those who were excluded due to excess movement are

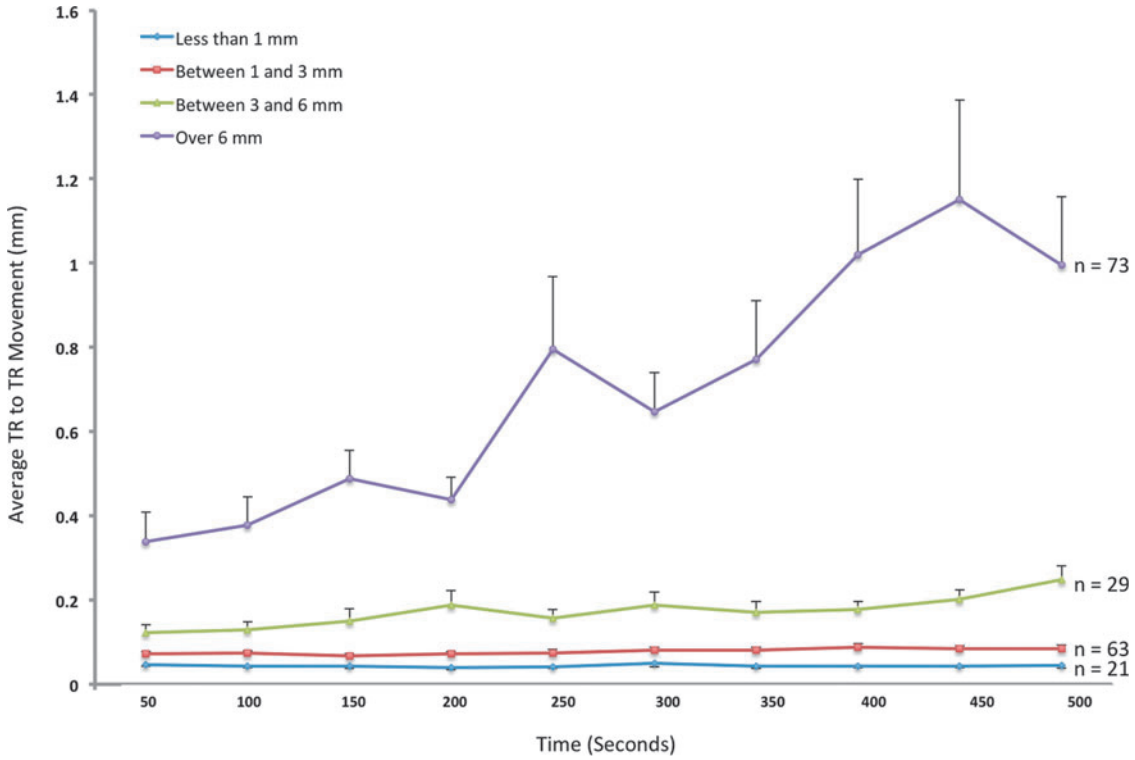

FIG. 1. Mean TR to TR movement over time. Each TR is 2 sec in duration and the mean TR-to-TR movement is averaged over blocks of 25 TRs (50 sec). The line reflecting movement ''Over 6 mm'' reflects all children, and each subsequent threshold reflects those children from the entire sample who have movement less than the threshold listed. Error bars reflect intersubject variability of the TR-to-TR movement. TR, repetition times. Color images available online at www.liebertpub.com/brain

provided in Table 1. The children scanned had a mean age of 7.1 years (SD ± 0.58) and the sex and handedness distribution between the groups were well balanced (Table 1). Between the group of children excluded due to movement artifacts and those included, there were no significant differences in age, sex, handedness, ethnicity, or family income (Table 1).

Functional brain networks and noise components

Eight of the 16 components matched brain networks found in the literature for children and adults. These networks are shown in Figure 2 and Supplementary Figure S1 (Supplementary Data are available online at www.liebertpub.com/brain) and include the DMN (Allen et al., 2011; Beckmann et al., 2005; Buckner et al., 2008; Damoiseaux et al., 2006; de Bie et al., 2012; Fair et al., 2008; Jolles et al., 2011; Raichle et al., 2001; Smith et al., 2009; Stevens et al., 2009), the left and right frontoparietal networks (Damoiseaux et al., 2006; Dosenbach et al., 2007; Fox et al., 2006; Jolles et al., 2011; Smith et al., 2009; Stevens et al., 2009; van den Heuvel and Hulshoff Pol, 2010), salience network (Seeley et al., 2007; Thomason et al., 2011), frontal network (Allen et al., 2011; de Bie et al., 2012; Smith et al., 2009; van den Heuvel and Hulshoff Pol, 2010), and the three primary sensory networks including the visual (Allen et al., 2011; Beckmann et al., 2005; Damoiseaux et al., 2006; de Bie et al., 2012; De Luca et al., 2006; Jolles et al., 2011; Smith et al., 2009; van den Heuvel and Hulshoff Pol, 2010), sensorimotor (Allen et al., 2011; Beckmann et al., 2005; Damoiseaux et al., 2006; de Bie et al., 2012; De Luca et al., 2006; Jolles et al., 2011; Smith et al., 2009; van den Heuvel and Hulshoff Pol, 2010), and auditory (Allen et al., 2011; Beckmann et al., 2005; Damoiseaux et al., 2006; de Bie et al., 2012; De Luca et al., 2006; Jolles et al., 2011; Mantini et al., 2007; Smith et al., 2009) networks. The frontal component is likely associated with the DFN, as when the threshold for this network is reduced, the posterior cingulate is included in the network. The parietal regions, however, do not emerge with lowering the threshold.

In addition, four noise components were also selected based on the spatial characteristics of these networks (Fig. 3 and Supplementary Fig. S2). The spatial patterns of these components reflected noise as a result of head motion, physiologic and flow artifacts, and correlations found in the cerebral spinal fluid. Finally, four additional components were identified as not consistently reported in the literature, but

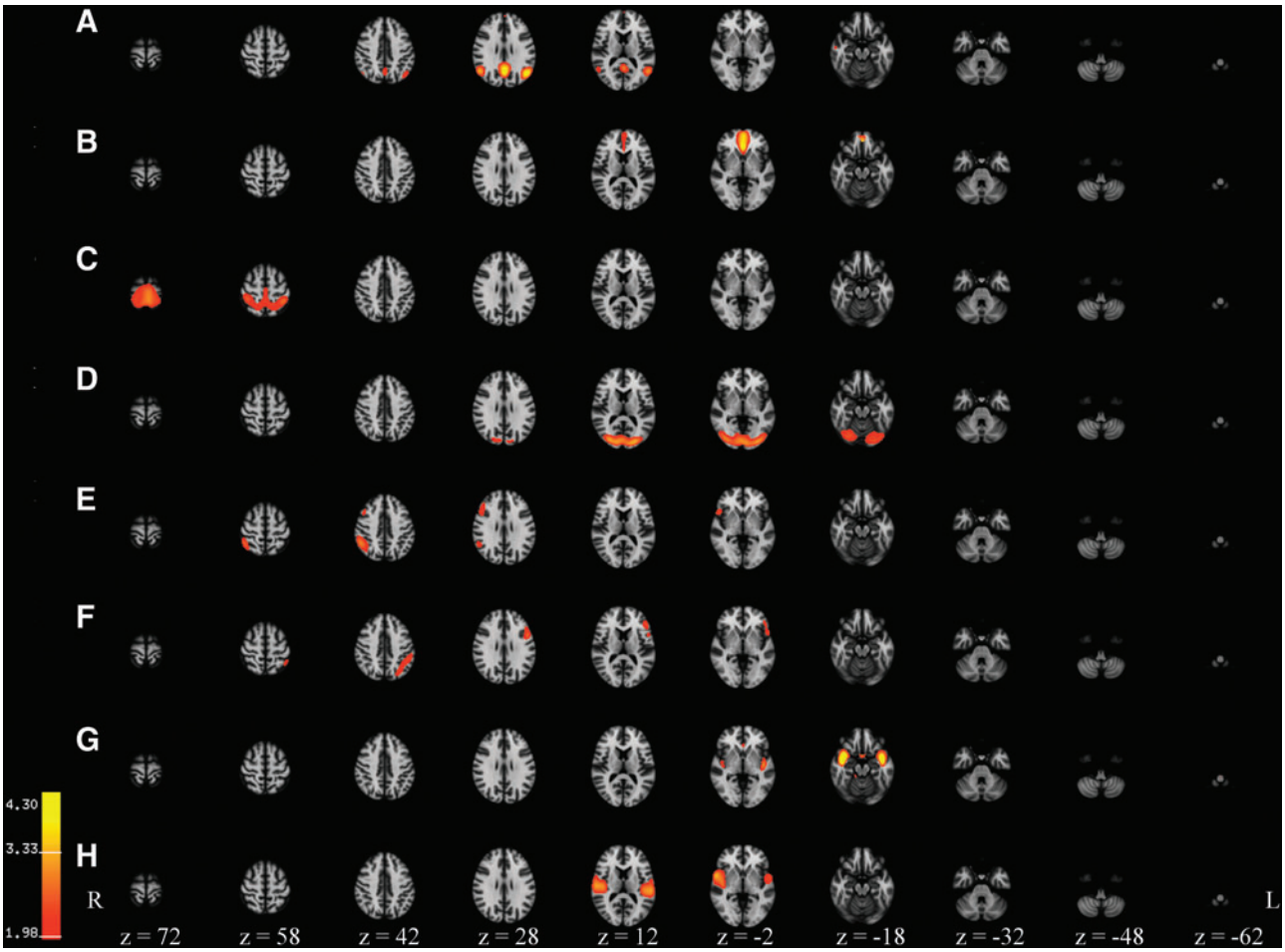

FIG. 2. Eight brain network components derived using independent component analysis in 84 children and a total sequence time of 8.2 min (246 TRs). The classification of the networks are **(A)** default mode network (DMN); **(B)** frontal network (likely component of anterior DMN); **(C)** sensorimotor network; **(D)** visual network; **(E)** right frontoparietal network; **(F)** left frontoparietal network; **(G)** salience network; **(H)** auditory network.

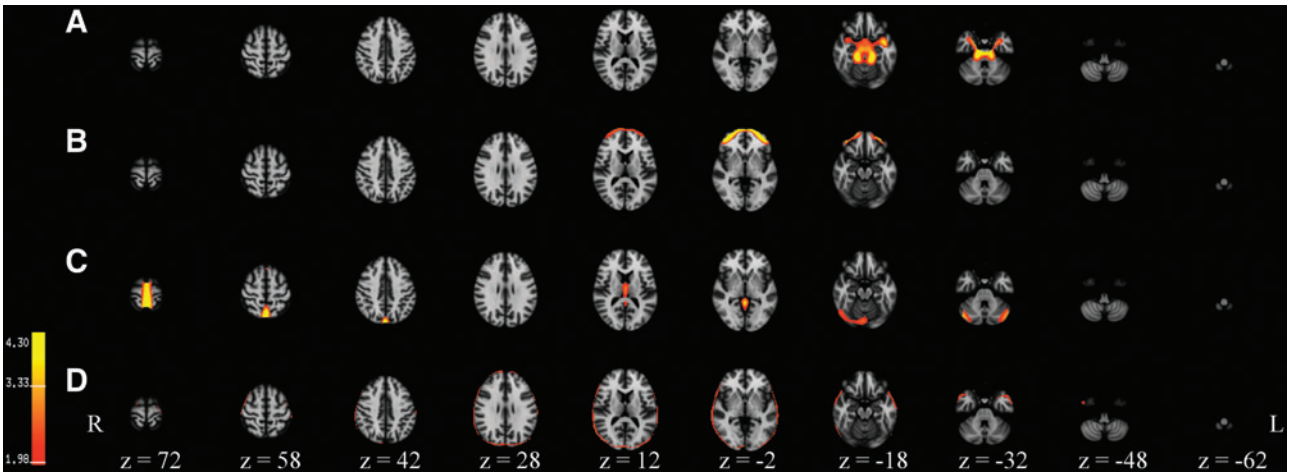

FIG. 3. Four noise network components extracted using independent component analysis in 84 children and a total sequence time of 8.2 min (246 TRs). The classification of the networks are **(A)** flow artifact; **(B)** frontal movement; **(C)** ventricular and midline movement; **(D)** ''ring of fire'' due to head motion.

also could not be classified as noise components. These components were excluded from the analyses.

Network stability over time

Network stability was measured by comparing the spatial overlap (φ) between individual ICA derived components from the full rs-fMRI image to the time-shortened rs-fMRI images, in which trailing volumes have been iteratively removed. Thus, Equation 1 determines how well ICA can derive spatial maps that are similar to the full rs-fMRI run, as the total length of the rs-fMRI run becomes shorter. The measure of spatial overlap is defined as the intersection over the union of two spatial maps, thus reflecting the same components derived with different amounts of time. Spatial maps that completely overlap (identical maps) have a value of 1, whereas spatial maps with

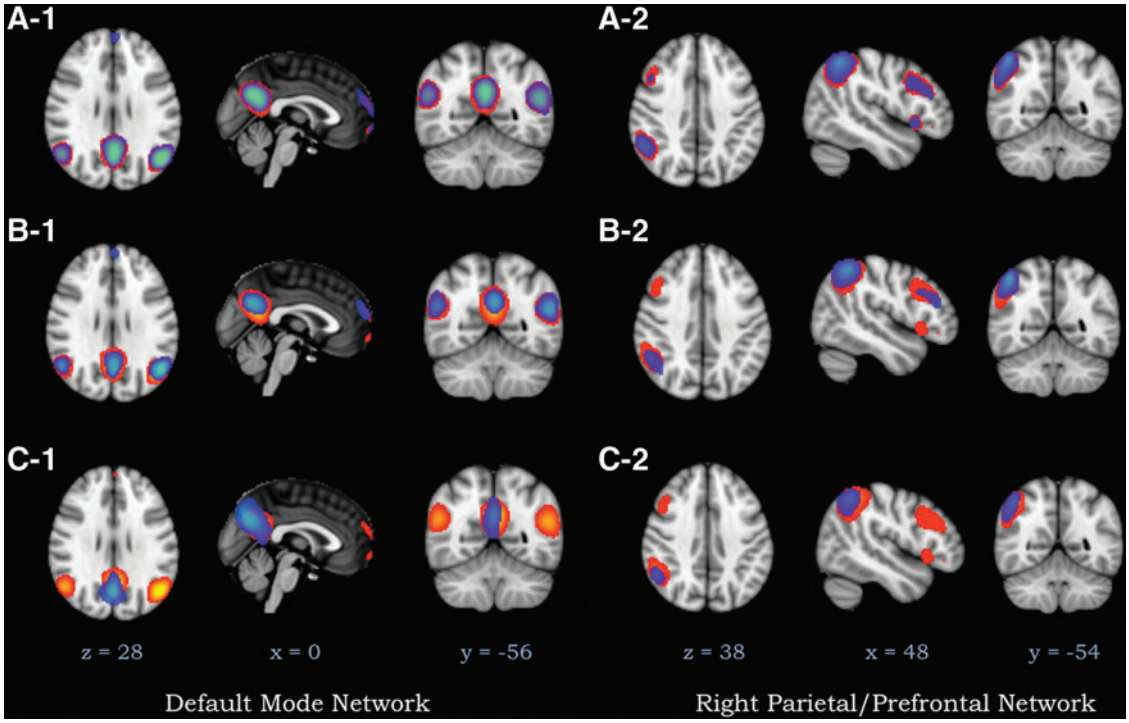

FIG. 4. Brain network stability of the default mode and right frontoparietal networks showing differences in the spatial overlap. Red reflects the networks calculated using the full 8.2 min resting-state sequence, whereas the blue networks show shorter periods of time. DMN: **(A-1)** Spatial overlap = 0.77 (collected with 4 min and 22 sec of data). **(B-1)** Spatial overlap = 0.54 (collected with 2 min and 12 sec of data); **(C-1)** Spatial overlap with = 0.25 (collected with 52 sec of data). *Right Frontoparietal Network:* **(A-2)** Spatial overlap = 0.76 (collected with 6 min and 32 sec of data). **(B-2)** Spatial overlap = 0.51 (collected with 3 min and 52 sec of data); **(C-2)** Spatial overlap with = 0.28 (collected with 1 min and 12 sec of data).

no overlap result in the value φ being zero. Since Equation 1 is nonlinear, we provide an example of the spatial overlap (φ) of the DMN using $\varphi \sim 0.75$, $\varphi \sim 0.5$, and $\varphi \sim 0.25$ (Fig. 4). The stability of the individual brain networks and noise networks are shown in Figure 5. Note that when $\varphi = 0.5$, there remains a high spatial overlap in the individual brain regions involved in the DMN. For two regions of equal size, a volume overlap of 50% translates into a φ of 0.33. Thus, we consider a $\varphi > 0.5$ a good level of spatial overlap.

We found that the spatial stability of the brain networks was quite high for 170 TRs and greater, equating to a total acquisition time greater than 5½ min (Fig. 5A). While we expected that the primary sensory components of auditory, visual, and sensorimotor would show the greatest stability, we found the greatest instability in the sensorimotor network. With the exception of the sensorimotor network, networks remained quite stable down to 3 min of acquisition time, at which point there was a steep decline in spatial overlap in most networks. Interestingly however, several brain networks, including the auditory and salience network remained quite stable down to 50 sec of acquisition time (25 TRs).

The spatial stability of the noise components was quite interesting (Fig. 5B). We tested whether noise components related to movement would show greater variability compared to the brain network components (Fig. 6). However, two noise components related to movement (Fig. 3B, D) were equally as stable as the brain networks (Fig. 5). Noise networks related to physiological noise also showed strikingly high spatial overlap with decreasing acquisition time. Overall, the noise components showed increasing spatial overlap with decreasing acquisition time compared to the brain network components, although a repeated measures ANOVA found only a trend level difference ($F_{(1,10)} = 4.46$, $p = 0.06$).

The dual regression approach showed results that were quite similar, with the auditory and salience network showing the highest level of stability over time (Supplementary Fig. S3). However, the decline in stability tended to be more linear and the comparison of the standard deviation shows an increase down to ~4 min of acquisition time, with a subsequent plateau (Supplementary Fig. S4). A reflection of the spatial overlap for the DMN for each individual is shown in Supplementary Figure S5).

Discussion

While the brains of children are highly similar to adult brains, there are also important developmental differences that make them quite distinct. There are differences in energy

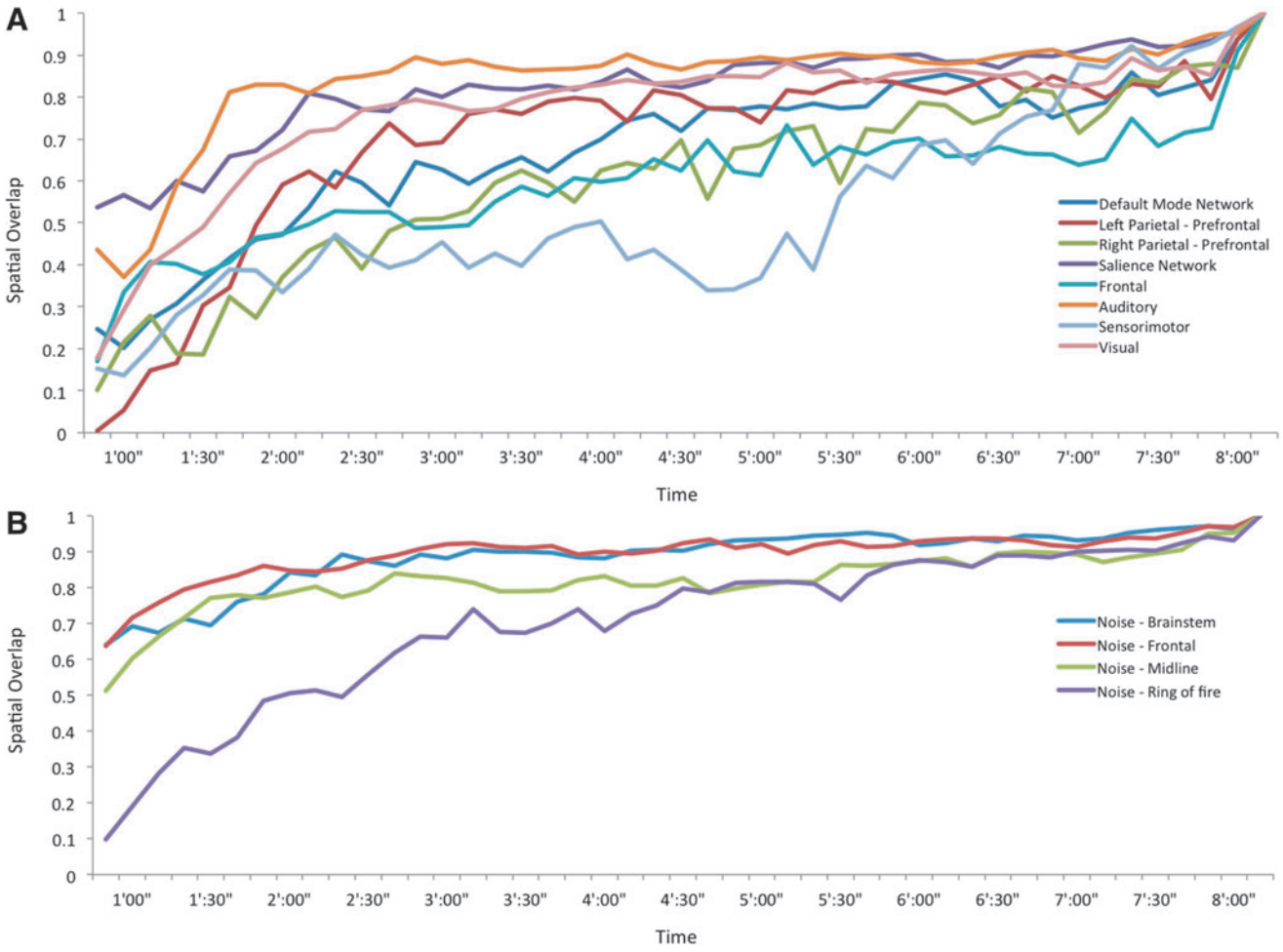

FIG. 5. Network stability of **(A)** Eight brain network components and **(B)** four noise components with respect to time of acquisition. Color images available online at www.liebertpub.com/brain

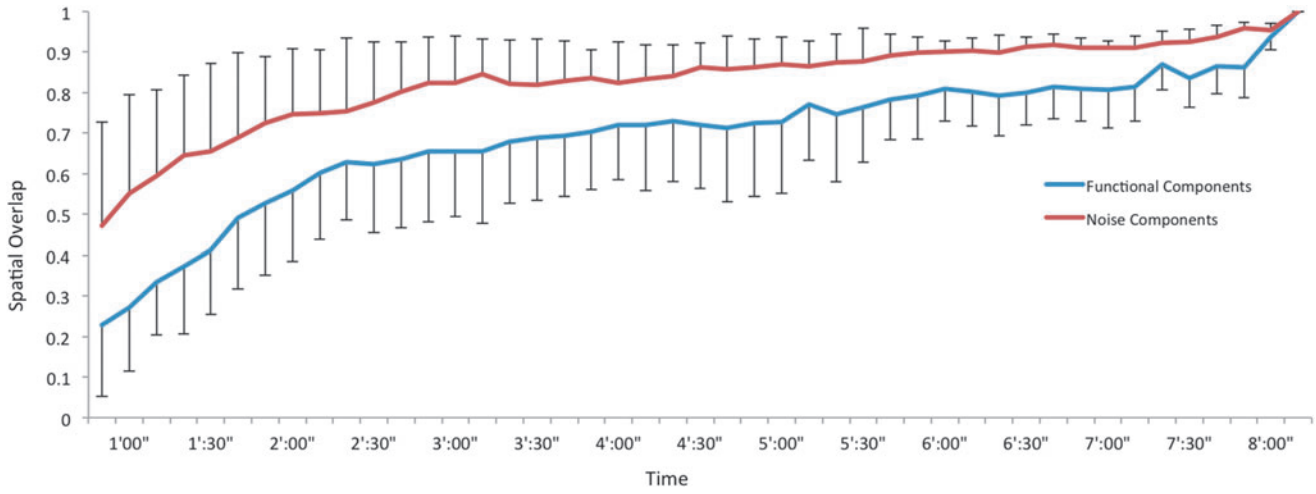

FIG. 6. Mean network stability of the eight brain network components and four noise components. Error bars are standard error of the mean. Color images available online at www.liebertpub.com/brain

metabolism and expenditure (Erecinska et al., 2004), gray and white matter volumes (Gogtay and Thompson, 2010; Lenroot and Giedd, 2006; Sowell et al., 2002), gyrification (White et al., 2010), functional connectivity (Fair et al., 2008, 2009; Jolles et al., 2011; Power et al., 2010; Stevens et al., 2009), and noise characteristics within the brain (McIntosh et al., 2010). Furthermore, physiological differences, such as heart and respiratory rates are also different between children and adults. Thus, without testing, it is unclear whether the optimal acquisition time of resting-state studies in adults (given a specific TR) can be directly translated to studies in children. While there is evidence that children show similar brain networks as those obtained in adults (de Bie et al., 2012; Fair et al., 2009; Gordon et al., 2011; Jolles et al., 2011; Langeslag et al., 2013; Stevens et al., 2009; Supekar et al., 2010; Thomason et al., 2011), the stability of these networks with respect to time of acquisition is not known. Thus, our primary goal was to test the network stability in resting-state fMRI in multiple brain networks in school-age children.

Using a TR of 2 sec, we found that scan acquisition times greater than 5½ min yielded very good network stability for all 8 brain components. Furthermore, we found that many of the brain networks had very good stability even with acquisition times as short as 3 min (Fig. 5). While studies in adults have found that the default mode and attention networks stabilize after ~5 to 6 min (Franco et al., 2013; Van Dijk et al., 2010), run lengths of 4 min have been shown to reliably estimate these brain networks (Van Dijk et al., 2010). Furthermore, adult studies have shown that global measures of small worldness can be reliably measured with acquisition times as short as 2 min (Whitlow et al., 2011). While our study suggests that the sensorimotor network stabilizes after 5½ min, the seven other brain networks remain quite stable down to 3 min of acquisition time. In fact, the auditory and salience networks remained stable with acquisition times as short as 50 sec. While the strength of a specific brain network certainly plays a role in the duration necessary to reliably measure that network, it is only a part of the story. Given equal amounts of noise, a highly connected but slowly oscillating network (cycling between correlated and uncorrelated time series) would show less connectivity in a shorter period of time compared to a less well connected but more rapidly oscillating network. Thus, one potential reason why certain networks show greater stability in time frames as short as 50 sec is that these brain networks cycle more frequently than other brain networks. To test this, we calculated the spectral density for the two most stable networks (auditory and salience networks) compared to two less stable networks (sensorimotor and frontal components). These are presented in Supplementary Figure S6. We also calculated normalized power within a low (0–0.05 Hz), medium (0.05–0.12 Hz), and high frequency (0.12–0.25 Hz) bands, similar to other studies (Baliki et al., 2011; Kim et al., 2014; Malinen et al., 2010). Indeed, a paired *t*-test showed that the power spectrum of auditory and salience networks show statistically significant greater power in the higher frequency range compared with the sensorimotor and frontal networks. However, the sensorimotor and frontal components show statistically significant greater power in the lower frequency range (Supplementary Fig. S6). While it is not surprising that two different networks show different frequency characteristics, the relative difference between high and low frequency power between the networks could contribute to the differences in network stability over time.

Since studies of acquisition times in adults have focused only on one or two specific brain networks, always including the DMN, direct comparisons of all the networks are difficult. Our findings of the DMN show that stability undergoes a gradual decline down to ~2½ min, after which there is a rapid drop in the spatial overlap measure (Fig. 5A). Thus, there is good correspondence in acquisition times between studies of children and adults with respect to the DMN.

Interestingly, we also found that four noise networks were also quite stable over time. While we expect that artifacts related to physiological changes in blood flow would show high stability, we expected networks related to movement to show greater instability. The two movement components; the frontal and ''ring of fire'' networks, involve movements that in our experience are characteristic for children who lie in the scanner. This is likely the reason for their high stability. The most common movement for individuals lying in the

scanner is rotation along the x-axis or similar to nodding the head ''yes.'' It is often difficult to securely restrain the head to prevent this type of movement. The ''ring of fire'' movement network involves an outer boundary of temporally correlated signal around the brain and defines movement in multiple directions. While this is less stable than the other noise networks, it is equally as stable as the brain networks. Since these noise networks remain relatively stable, they will be easier to identify using algorithms designed for automated network detection (Storti et al., 2013).

There are several limitations to the current study. First, approximately half of our subjects were dropped due to excessive movement over the 8 min 20 sec run. Significant movement in the MRI in young children is common and we found no difference in demographic variables between the children included and those excluded due to motion. Since we found evidence for increased movement over time in the children who were excluded, shorter acquisition times would reduce the number of children excluded as a result of motion. In addition, our movement criteria were more stringent than some other studies (de Bie et al., 2012; Gordon et al., 2011) and resulted in approximately half of our subjects being dropped due to motion. This resulted in including only children who were able to remain very still and raises the question as to whether our findings generalize to all children. Second, we fixed the dimensionality at 16, as we found in a prior study that this level of dimensionality provided components similar to those seen in adult studies (Langeslag et al., 2013). In the extremes, differences in dimensionality will have large effects on network stability (i.e., 1 brain network will show excellent stability, whereas 200 brain networks would be much more unstable). There is evidence that using similar levels of dimensionality, brain networks in children become more fragmented into multiple networks compared to adults (de Bie et al., 2012). Thus, our choice of 16 components in school-age children was selected on the basis of our prior work. Third, the advent of multiband sequences will greatly enhance the number of volumes collected within a specific time period (Moeller et al., 2010). The higher sampling rate will allow for increased signal to noise and better detection of physiological confounds and thus may decrease the optimal acquisition time for network stability. However, comparisons of acquisition times between multiband sequences and those with traditional TRs have both shown stabilization after 5 to 6 min (Liao et al., 2013). This suggests that brain network stability is more related to duration of acquisition than sampling rate. Finally, since different brain networks show different levels of stability, our study may have relevance with respect to sliding window approaches of connectivity (Chang and Glover, 2010; Sakoglu et al., 2010). For example, brain networks that show high stability in short periods of time, such as the auditory and salience networks may require shorter periods of the sliding window than other networks. Further studies, especially those that include multiband imaging are important to address this question.

Conclusions

In conclusion, we found that component group maps of all brain networks stabilized after $\sim$5½ min of data acquisition in school-age children. While some components such as the auditory and salience networks remained relatively stable down to acquisition times of less than 2 min (Fig. 5), other networks show considerable less stability. The sensorimotor network, for example, was the least stable brain network. Since the signal to noise of extracting network components increases by the square root of the run length (Van Dijk et al., 2010), increasing the acquisition time allows for a greater number of sampling points and a better capture of the time series. However, there is a trade off since increasing the acquisition time also results in an increased burden for the children and the risk of increasing motion and other artifacts. This is especially important since it has been shown that subject motion artifacts can influence functional connectivity patterns within the brain (Power et al., 2012). Thus, our findings suggest that an acquisition time of $\sim$5½ min is sufficient to capture a comprehensive set of brain networks. Since it has been shown that seed-based methods and ICA yield similar results for some of the well-studied brain networks indicates that these complementary methods extract similar signals (Calhoun et al., 2012; Van Dijk et al., 2010). This suggests that our findings are likely to apply to seed-based approaches.

Acknowledgments

The study was supported by ZonMw TOP 40-00812-98-11021. The Generation R Study is conducted by the Erasmus Medical Center in close collaboration with the Erasmus University Rotterdam, the Municipal Health Service in the Rotterdam area, the Rotterdam Homecare Foundation, Rotterdam, and the Stichting Trombosedienst & Artsenlaboratorium Rijnmond (STAR-MDC), Rotterdam. We gratefully acknowledge the contribution of children and parents, general practitioners, hospitals, midwives, and pharmacies in Rotterdam. We also gratefully acknowledge the hard work of the postdocs and PhD students who have assisted with data collection. These include Hanan El Marroun, Ilse Nijs, Nikita Schoemaker, Sabine Mous, Gerbrich van den Bosch, Sandra Thijssen, Andrea Wildeboer, Laura Blanken, Carolyn Langen, and Akvile Lukose. Neuroimaging studies within the Generation R have additional support through the European Community's 7th Framework Programme (FP7/2008–2013) under grant agreement 212652 (NUTRIMENTHE) and the Stichting Sophia Kinderziekenhuis Fonds. The Generation R Study is made possible by financial support from the Erasmus Medical Center, Rotterdam, the Erasmus University Rotterdam, ZonMw (ZonMW 10.000.1003), the Netherlands Organization for Scientific Research (NWO), the Ministry of Health, Welfare and Sport, and the Ministry of Youth and Families.

Author Disclosure Statement

No competing financial interests exist.

References

Allen EA, Erhardt EB, Damaraju E, Gruner W, Segall JM, Silva RF, et al. 2011. A baseline for the multivariate comparison of resting-state networks. Front Syst Neurosci 5:2.

Baliki MN, Baria AT, Apkarian AV. 2011. The cortical rhythms of chronic back pain. J Neurosci 31:13981–13990.

Beckmann CF, DeLuca M, Devlin JT, Smith SM. 2005. Investigations into resting-state connectivity using independent

component analysis. Philos Trans R Soc Lond B Biol Sci 360:1001–1013.
Beckmann CF, Mackay CE, Filippini N, Smith SM. 2009. Group comparison of resting-state FMRI data using multi-subject ICA and dual regression. In: *Human Brain Mapping 15th Annual Meeting San Francisco*. CA: Organization for Human Brain Mapping.
Biswal B, Yetkin FZ, Haughton VM, Hyde JS. 1995. Functional connectivity in the motor cortex of resting human brain using echo-planar MRI. Magn Reson Med 34:537–541.
Buckner RL, Andrews-Hanna JR, Schacter DL. 2008. The brain's default network: anatomy, function, and relevance to disease. Ann N Y Acad Sci 1124:1–38.
Calhoun VD, Adali T. 2012. Multisubject independent component analysis of fMRI: a decade of intrinsic networks, default mode, and neurodiagnostic discovery. IEEE Rev Biomed Eng 5:60–73.
Calhoun VD, Adali T, Pearlson GD, Pekar JJ. 2001. A method for making group inferences from functional MRI data using independent component analysis. Hum Brain Mapp 14:140–151.
Calhoun VD, Eichele T, Adali T, Allen EA. 2012. Decomposing the brain: components and modes, networks and nodes. Trends Cogn Sci 16:255–256.
Chang C, Glover GH. 2010. Time-frequency dynamics of resting-state brain connectivity measured with fMRI. Neuroimage 50:81–98.
Cox RW. 2012. AFNI: what a long strange trip it's been. Neuroimage 62:743–747.
Damoiseaux JS, Rombouts SA, Barkhof F, Scheltens P, Stam CJ, Smith SM, et al. 2006. Consistent resting-state networks across healthy subjects. Proc Natl Acad Sci U S A 103: 13848–13853.
de Bie HM, Boersma M, Adriaanse S, Veltman DJ, Wink AM, Roosendaal SD, et al. 2012. Resting-state networks in awake five- to eight-year old children. Hum Brain Mapp 33:1189–1201.
De Luca M, Beckmann CF, De Stefano N, Matthews PM, Smith SM. 2006. fMRI resting state networks define distinct modes of long-distance interactions in the human brain. Neuroimage 29:1359–1367.
Dosenbach NU, Fair DA, Miezin FM, Cohen AL, Wenger KK, Dosenbach RA, et al. 2007. Distinct brain networks for adaptive and stable task control in humans. Proc Natl Acad Sci U S A 104:11073–11078.
Erecinska M, Cherian S, Silver IA. 2004. Energy metabolism in mammalian brain during development. Prog Neurobiol 73: 397–445.
Fair DA, Cohen AL, Dosenbach NU, Church JA, Miezin FM, Barch DM, et al. 2008. The maturing architecture of the brain's default network. Proc Natl Acad Sci U S A 105:4028–4032.
Fair DA, Cohen AL, Power JD, Dosenbach NU, Church JA, Miezin FM, et al. 2009. Functional brain networks develop from a ''local to distributed'' organization. PLoS Comput Biol 5:e1000381.
Fox MD, Corbetta M, Snyder AZ, Vincent JL, Raichle ME. 2006. Spontaneous neuronal activity distinguishes human dorsal and ventral attention systems. Proc Natl Acad Sci U S A 103:10046–10051.
Franco AR, Mannell MV, Calhoun VD, Mayer AR. 2013. Impact of analysis methods on the reproducibility and reliability of resting-state networks. Brain Connect 3:363–374.
Gogtay N, Thompson PM. 2010. Mapping gray matter development: implications for typical development and vulnerability to psychopathology. Brain Cogn 72:6–15.
Gordon EM, Lee PS, Maisog JM, Foss-Feig J, Billington ME, Vanmeter J, et al. 2011. Strength of default mode resting-state connectivity relates to white matter integrity in children. Dev Sci 14:738–751.
Jaddoe VW, Mackenbach JP, Moll HA, Steegers EA, Tiemeier H, Verhulst FC, et al. 2006. the Generation R Study: design and cohort profile. Eur J Epidemiol 21:475–484.
Jenkinson M, Bannister P, Brady M, Smith S. 2002. Improved optimization for the robust and accurate linear registration and motion correction of brain images. Neuroimage 17:825–841.
Jenkinson M, Beckmann CF, Behrens TE, Woolrich MW, Smith SM. 2012. FSL. Neuroimage 62:782–790.
Jenkinson M, Smith S. 2001. A global optimisation method for robust affine registration of brain images. Med Image Anal 5:143–156.
Jolles DD, van Buchem MA, Crone EA, Rombouts SA. 2011. A comprehensive study of whole-brain functional connectivity in children and young adults. Cereb Cortex 21:385–391.
Kim J, Van Dijk KR, Libby A, Napadow V. 2014. Frequency-dependent relationship between resting-state functional magnetic resonance imaging signal power and head motion is localized within distributed association networks. Brain Connect 4:30–39.
Kung CC, Peissig JJ, Tarr MJ. 2007. Is region-of-interest overlap comparison a reliable measure of category specificity? J Cogn Neurosci 19:2019–2034.
Langeslag SJ, Schmidt M, Ghassabian A, Jaddoe VW, Hofman A, van der Lugt A, et al. 2013. Functional connectivity between parietal and frontal brain regions and intelligence in young children: the Generation R study. Hum Brain Mapp 34:3299–3307.
Lenroot RK, Giedd JN. 2006. Brain development in children and adolescents: insights from anatomical magnetic resonance imaging. Neurosci Biobehav Rev 30:718–729.
Liao XH, Xia MR, Xu T, Dai ZJ, Cao XY, Niu HJ, et al. 2013. Functional brain hubs and their test-retest reliability: a multiband resting-state functional MRI study. Neuroimage 83: 969–982.
Malinen S, Vartiainen N, Hlushchuk Y, Koskinen M, Ramkumar P, Forss N, et al. 2010. Aberrant temporal and spatial brain activity during rest in patients with chronic pain. Proc Natl Acad Sci U S A 107:6493–6497.
Mantini D, Perrucci MG, Del Gratta C, Romani GL, Corbetta M. 2007. Electrophysiological signatures of resting state networks in the human brain. Proc Natl Acad Sci U S A 104: 13170–13175.
McIntosh AR, Kovacevic N, Lippe S, Garrett D, Grady C, Jirsa V. 2010. The development of a noisy brain. Arch Ital Biol 148:323–337.
Moeller S, Yacoub E, Olman CA, Auerbach E, Strupp J, Harel N, et al. 2010. Multiband multislice GE-EPI at 7 tesla, with 16-fold acceleration using partial parallel imaging with application to high spatial and temporal whole-brain fMRI. Magn Reson Med 63:1144–1153.
Power JD, Barnes KA, Snyder AZ, Schlaggar BL, Petersen SE. 2012. Spurious but systematic correlations in functional connectivity MRI networks arise from subject motion. Neuroimage 59:2142–2154.
Power JD, Fair DA, Schlaggar BL, Petersen SE. 2010. The development of human functional brain networks. Neuron 67:735–748.
Raichle ME, MacLeod AM, Snyder AZ, Powers WJ, Gusnard DA, Shulman GL. 2001. A default mode of brain function. Proc Natl Acad Sci U S A 98:676–682.

Sakoglu U, Pearlson GD, Kiehl KA, Wang YM, Michael AM, Calhoun VD. 2010. A method for evaluating dynamic functional network connectivity and task-modulation: application to schizophrenia. Magma 23:351–366.

Satterthwaite TD, Wolf DH, Loughead J, Ruparel K, Elliott MA, Hakonarson H, et al. 2012. Impact of in-scanner head motion on multiple measures of functional connectivity: relevance for studies of neurodevelopment in youth. Neuroimage 60:623–632.

Seeley WW, Menon V, Schatzberg AF, Keller J, Glover GH, Kenna H, et al. 2007. Dissociable intrinsic connectivity networks for salience processing and executive control. J Neurosci 27:2349–2356.

Smith SM, Fox PT, Miller KL, Glahn DC, Fox PM, Mackay CE, et al. 2009. Correspondence of the brain's functional architecture during activation and rest. Proc Natl Acad Sci U S A 106:13040–13045.

Sowell ER, Trauner DA, Gamst A, Jernigan TL. 2002. Development of cortical and subcortical brain structures in childhood and adolescence: a structural MRI study. Dev Med Child Neurol 44:4–16.

Stevens MC, Pearlson GD, Calhoun VD. 2009. Changes in the interaction of resting-state neural networks from adolescence to adulthood. Hum Brain Mapp 30:2356–2366.

Storti SF, Formaggio E, Nordio R, Manganotti P, Fiaschi A, Bertoldo A, et al. 2013. Automatic selection of resting-state networks with functional magnetic resonance imaging. Front Neurosci 7:72.

Supekar K, Uddin LQ, Prater K, Amin H, Greicius MD, Menon V. 2010. Development of functional and structural connectivity within the default mode network in young children. Neuroimage 52:290–301.

Tellegen P, Wijnberg-Williams B, Laros J. 2005. Snijders-Oomen Niet-Verbale Intelligentietest: SON-R 2½ -7. Amsterdam: Boom Testuitgevers.

Thomason ME, Dennis EL, Joshi AA, Joshi SH, Dinov ID, Chang C, et al. 2011. Resting-state fMRI can reliably map neural networks in children. Neuroimage 55:165–175.

Tiemeier H, Velders FP, Szekely E, Roza SJ, Dieleman G, Jaddoe VW, et al. 2012. The Generation R Study: a review of design, findings to date, and a study of the 5-HTTLPR by environmental interaction from fetal life onward. J Am Acad Child Adolesc Psychiatry 51:1119–1135.e1117.

Uddin LQ. 2011. Resting-state FMRI and developmental systems neuroscience. Front Neurosci 5:14.

van den Bosch GE, Marroun HE, Schmidt MN, Tibboel D, Manoach DS, Calhoun VD, et al. 2014. Brain connectivity during verbal working memory in children and adolescents. Hum Brain Mapp 35:698–711.

van den Heuvel MP, Hulshoff Pol HE. 2010. Exploring the brain network: a review on resting-state fMRI functional connectivity. Eur Neuropsychopharmacol 20:519–534.

Van Dijk KR, Hedden T, Venkataraman A, Evans KC, Lazar SW, Buckner RL. 2010. Intrinsic functional connectivity as a tool for human connectomics: theory, properties, and optimization. J Neurophysiol 103:297–321.

Van Dijk KR, Sabuncu MR, Buckner RL. 2012. The influence of head motion on intrinsic functional connectivity MRI. Neuroimage 59:431–438.

Vogel AC, Power JD, Petersen SE, Schlaggar BL. 2010. Development of the brain's functional network architecture. Neuropsychol Rev 20:362–375.

White T, Hongwanishkul D, Schmidt M. 2011. Increased anterior cingulate and temporal lobe activity during visuospatial working memory in children and adolescents with schizophrenia. Schizophr Res 125:118–128.

White T, Marroun HE, Nijs I, Schmidt M, van der Lugt A, Wielopolki PA, et al. 2013. Pediatric population-based neuroimaging and the Generation R Study: the intersection of developmental neuroscience and epidemiology. Eur J Epidemiol 28:99–111.

White T, Moeller S, Schmidt M, Pardo JV, Olman C. 2012. Evidence for intact local connectivity but disrupted regional function in the occipital lobe in children and adolescents with schizophrenia. Hum Brain Mapp 33:1803–1811.

White T, O'Leary D, Magnotta V, Arndt S, Flaum M, Andreasen NC. 2001. Anatomic and functional variability: the effects of filter size in group fMRI data analysis. Neuroimage 13: 577–588.

White T, Su S, Schmidt M, Kao CY, Sapiro G. 2010. The development of gyrification in childhood and adolescence. Brain Cogn 72:36–45.

Whitlow CT, Casanova R, Maldjian JA. 2011. Effect of resting-state functional MR imaging duration on stability of graph theory metrics of brain network connectivity. Radiology 259:516–524.

Wu K, Taki Y, Sato K, Hashizume H, Sassa Y, Takeuchi H, et al. 2013. Topological organization of functional brain networks in healthy children: differences in relation to age, sex, and intelligence. PLoS One 8:e55347.

Zadeh LA. 1965. Fuzzy sets. Inf Control 8:338–353.

Zhong J, Rifkin-Graboi A, Ta AT, Yap KL, Chuang KH, Meaney MJ, et al. 2014. Functional networks in parallel with cortical development associate with executive functions in children. Cereb Cortex 24:1937–1947.

Address correspondence to:
Tonya White
Department of Child and Adolescent Psychiatry
Erasmus University Medical Centre—Sophia
Children's Hospital
Kamer SP-2869
Postbus 2060
3000 CB Rotterdam
Netherlands

E-mail: t.white@erasmusmc.nl